Electrochimica Acta, 1965, Vol. 10, pp. 1117 to 1126. Pergamon Press Ltd. Printed in Northern Ireland

THE ANODIC PROCESSES IN ALUMINIUM CELLS*

R. PIONTELLI, B. MAZZA and P. PEDEFERRI
Laboratorio del gruppo di ricerca "Elettroliti e processi elettrochimici" del C.N.R.,
Institute for Electrochemistry, Physical Chemistry and Metallurgy,
Milan Polytechnic, Milan, Italy

Abstract—Systematic work on the anode processes at carbon electrodes in cryolite melts with various alumina contents at 1050°C has been carried out. The behaviour of anodes of different shape and size has been investigated.

The phenomenological laws followed by the apparent anode overvoltage before the onset of the anode effect have been determined and the different contributions have been analysed.

The circumstances of the onset and some of the main aspects of the anode effect have been analysed. The whole matter is briefly discussed.

Résumé—On a accompli des recherches systématiques sur le comportement anodique d'électrodes de carbone de différentes géométries et dimensions en bains de cryolithe, avec de différentes teneurs d'alumine, à 1050°C.

On a déterminé les lois phénoménologiques suivies par les surtensions anodiques apparentes avant l'intervention de l'effet anodique et on a analysé les différentes contributions.

On a étudié systématiquement les conditions d'intervention et les aspects les plus essentiels de l'effet anodique. On discute brièvement l'ensemble des résultats expérimentaux.

Zusammenfassung—Es wurde eine systematische Untersuchung über die Anodenvorgänge an Graphitelektroden verschiedener Form und Grösse in Kryolith-Schmelzen mit variiertem Tonerdegehalt bei 1050°C durchgeführt.

Die für die scheinbare Anodenüberspannung vor dem Einsetzen des Anodeneffekts geltenden phänomenologischen Gesetzmässigkeiten wurden ermittelt und die Überspannungswerte in die verschiedenen Anteile zerlegt.

Man untersuchte die Bedingungen für das Einsetzen des Anodeneffekts und einige seiner Haupterscheinungen. Die experimentellen Resultate werden zusammenfassend diskutiert.

WORK carried out in our laboratory on the polarization phenomena in galvanic cells with fused electrolytes, particularly in the aluminium cell,[1] has enabled us to throw light on some less known aspects of the anodic phenomena.

There have been many studies in this field, on overvoltage[2] and the "anode effect",[3] but neither a satisfactory knowledge of the phenomenological laws, nor a consistent explanation of them, has yet been obtained.

EXPERIMENTAL TECHNIQUE AND RESULTS

The characteristics of the polarization cell and those of the reference electrode (RE: Al/Na_3AlF_6 sat. Al_2O_3), the shapes of the anodes and the diagram of the circuit are given in Figs. 1, 2 and 3. A graphite RE was also used, checked with the RE above.

The electrical supply to the cell in the overvoltage measurements was in the form of rectangular current pulses, whose intensity, duration and pauses could be varied at will; in the study of the anode effect phenomena the current intensity was also increased or decreased continuously. The voltage outputs of the cell formed by the

* Presented at the 15th meeting of CITCE, London, September 1964; manuscript received 3 November 1964.

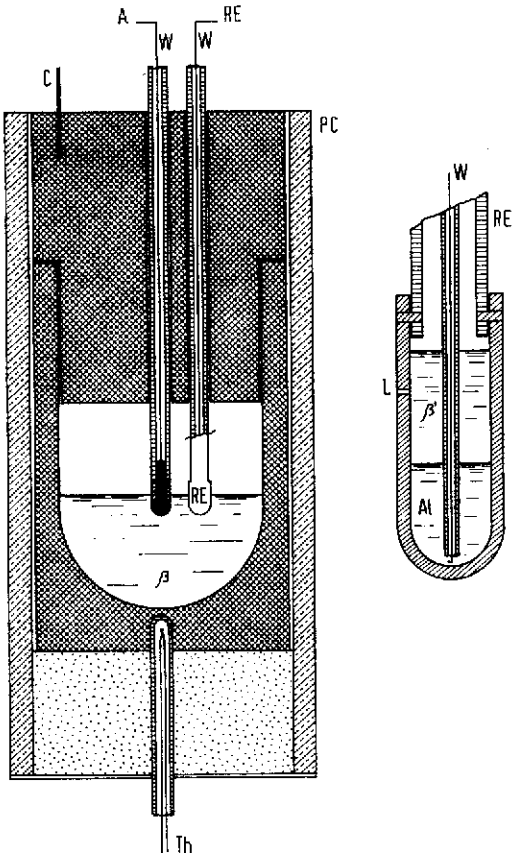

FIG. 1. Polarization cell (hemispherical symmetry) and reference electrode (RE: Al/Na_3AlF_6 sat. Al_2O_3); (sectional views).

A, anode; C, cathode; W, tungsten wire; Th, thermocouple; β, bath; β^1, bath of Na_3AlF_6 sat. Al_2O_3; Al, molten aluminium; L, channel for the interliquid junction.

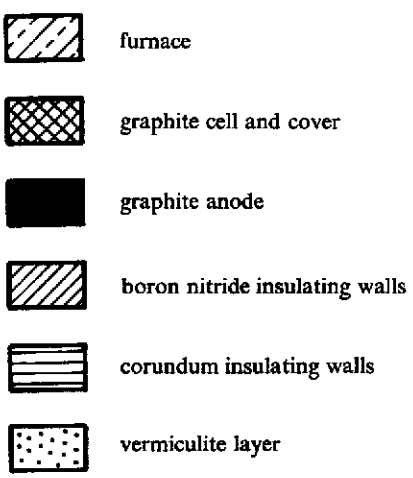

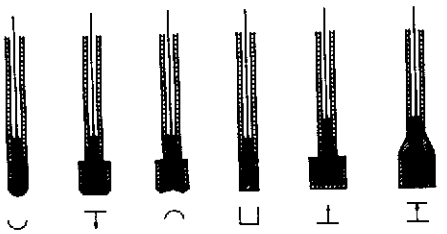

FIG. 2. Shapes of the anodes, with their symbols. From the left: hemispherical, horizontal downwards, concave, cylindrical, horizontal upwards and horizontal upwards with shield anodes.

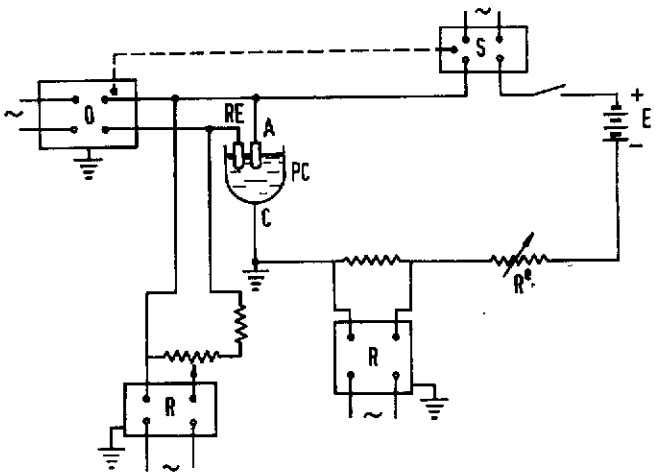

FIG. 3. Circuit diagram.
E, batteries (emf ≃ 75V);
S, electronic (10^{-5} s) or electronically operated mechanical switch (10^{-3} s);
O, Tektronix cathode-ray oscilloscope (0·5 ms/cm) with Robot camera;
R, Leeds and Northrup Speedomax recorder (30 s/in);
R^e, rheostat (0–1100 Ω).

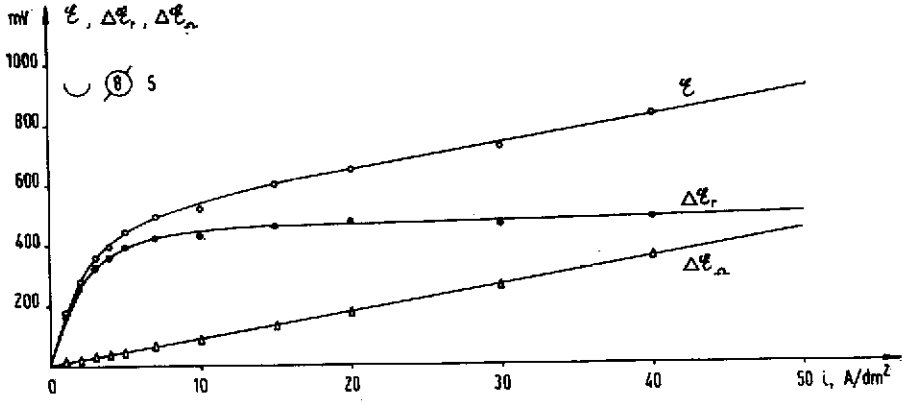

FIG. 4. Overvoltage *vs* current density. 1050°C. In this figure and in those following, the first number after the symbolic indication of the anode shape gives the anode diameter in mm (○), or the anode area in cm² (□); the second number gives the wt-% of Al_2O_3 (referred to Na_3AlF_6) of the baths.

anode to be investigated and the RE above were recorded before, during and after current flow.

The following materials were used: natural cryolite; alumina of analytical reagent grade; graphite for nuclear grade; boron nitride (U.S.A.).

As regards overvoltage effects, the influence of current density, anode shape and size, Al_2O_3 content of the baths, mechanical vibration impressed on the anodes, have been investigated.

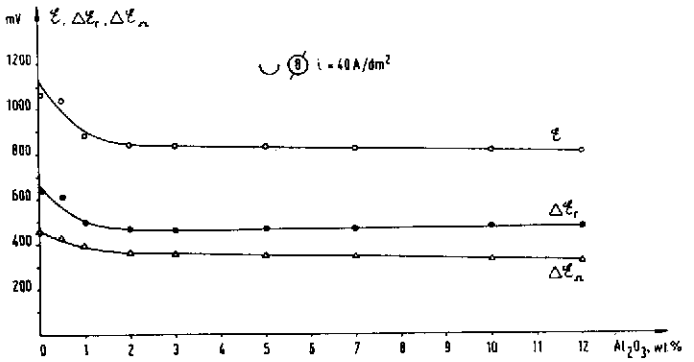

FIG. 5. Overvoltage *vs* wt-% Al_2O_3. 1050°C.

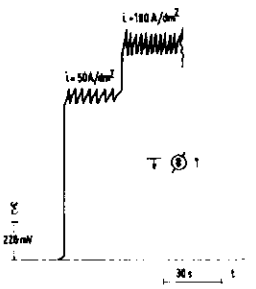

FIG. 6. Oscillations in apparent overvoltage for horizontal (downwards) or concave anodes. 1050°C.

The influence of current density and Al_2O_3 content is already well known (Figs. 4 and 5).

The other main experimental results can be summarized as follows.

1. The "apparent overvoltage" is approximately constant with time for hemispherical and cylindrical anodes; but on the contrary, it shows rhythmical oscillations for the horizontal (downwards) and concave anodes (Fig. 6).
2. Fast oscillographic recordings of the anode voltage at the closing and the opening of the circuit (Fig. 7) show that the "jump" at closing, which corresponds to the ohmic drop in the bath between anode and RE, is smaller (about 7–10 times) than the jump at opening, which includes also a supplementary ohmic drop due to the presence of gas in the anode region. Both jumps are proportional to the current intensity (Fig.8). Moreover, for given current intensity, the values of the jump at opening decrease with the increasing Al_2O_3 content (Figs. 8 and 5).
3. The "apparent overvoltage" ($\mathscr{E}$) can thus be divided (Fig. 7) into a first term ($\Delta\mathscr{E}_\Omega$), measured by the voltage jump at opening (effective ohmic drop voltage), and a

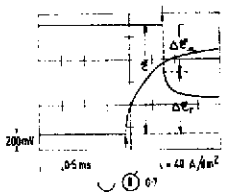

FIG. 7. Oscillographic recording of anode voltage. 1050°C.
↑ start of the rectangular current pulse; ↓ end of the pulse.

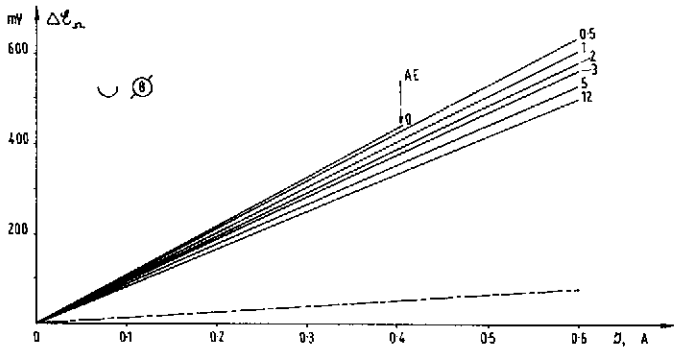

FIG. 8. Voltage jump at break *vs* current intensity, for various wt-% Al_2O_3. 1050°C. The dashed straight line gives the voltage jump at make. AE = anode effect.

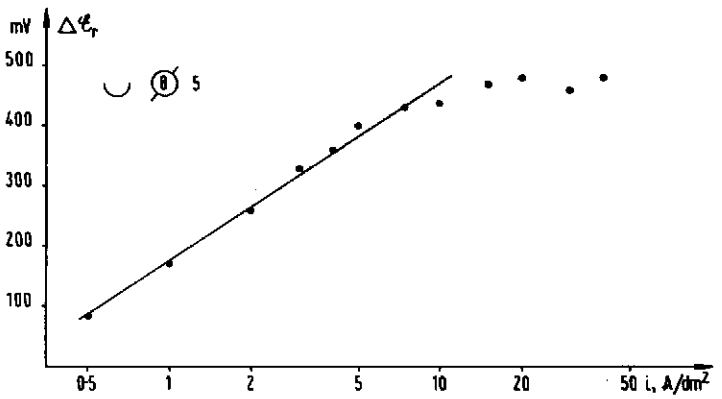

FIG. 9. Residual overvoltage *vs* log (current density). 1050°C. Tafel constants: *a*, 175 mV; *b*, 290 mV.

second term of residual overvoltage $\Delta\mathscr{E}_r$, which follows the Tafel law, in the current density range between 0·5 and 5–7 A/dm² (Fig. 9). Also, the residual overvoltage decreases, for given current density, with the increasing Al_2O_3 content (Fig. 5).

4. Slow recording of the anode voltage after the current break enables us to divide the residual overvoltage into two contributions. A first contribution, in the order of 230 mV at 40 A/dm², disappears in a very short time (in the order of a fraction of a second), and can be interpreted as a part of the overvoltage of the electrode processes. A second contribution, on the contrary, shows a greater persistence in

time and corresponds to a slower relaxation of the chemical configuration, both at the electrode surface and in the bath.

The contribution of the overvoltage of the electrode processes to the residual overvoltage can be attributed to an excess (with reference to equilibrium) of the thermodynamic level of the oxygen, in whatever form (ionic or atomic, adsorbed or of surface compound) that is potential determining for the anode under the considered conditions. Its amount cannot depend only on the displacement from equilibrium of the CO_2/CO ratio in the gas developed at the anode. For high values of the ratio current density/$Al_2O_3^-$ content, it seems likely that fluorine compounds at the anode surface produce inhibition of oxidation.

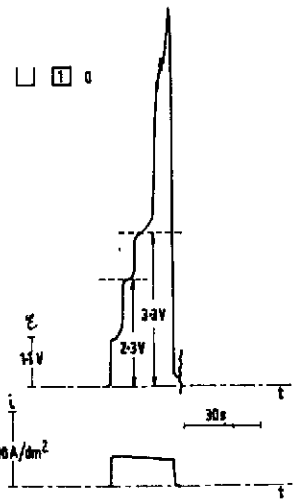

FIG. 10. Anode voltage, showing the characteristic "steps" before the onset of the AE for baths poor in Al_2O_3. 1050°C.

5. Mechanical vibration impressed on the anode lowers the apparent overvoltage (other factors being equal), and eliminates the typical oscillations at horizontal (downwards) and concave anodes. Moreover it causes a decrease of 60–80 mV of the most slowly time-dependent part of the residual overvoltage. This decrease gives a lower limit of the concentration polarization.

With baths poor in Al_2O_3, and high enough current densities, the anodic voltage presents two steps, up to about 2 and about 3V respectively, before the onset of the "anode effect" (AE) (Fig. 10).

The main phenomenological aspects of the AE and the conditions of its onset, permanence and disappearance have been investigated, especially the influence on the critical current intensity ($\mathscr{I}_c$) of bath composition (Al_2O_3 content and "acidity"), anode shape and size, bath temperature, mechanical vibration impressed on the anodes, history of the anodes, and the current/increasing law.

For anodes of identical shape and surface state, $\mathscr{I}_c$ is a function of the electrode apparent area according to a law which is not of simple proportionality, and therefore it is impossible to define a critical value of current density, for a given anode shape.

The influence of the Al_2O_3 content on the critical current intensity is represented in Fig. 11, for the different shapes and sizes of the anodes. The values of $\mathscr{I}_c$ are

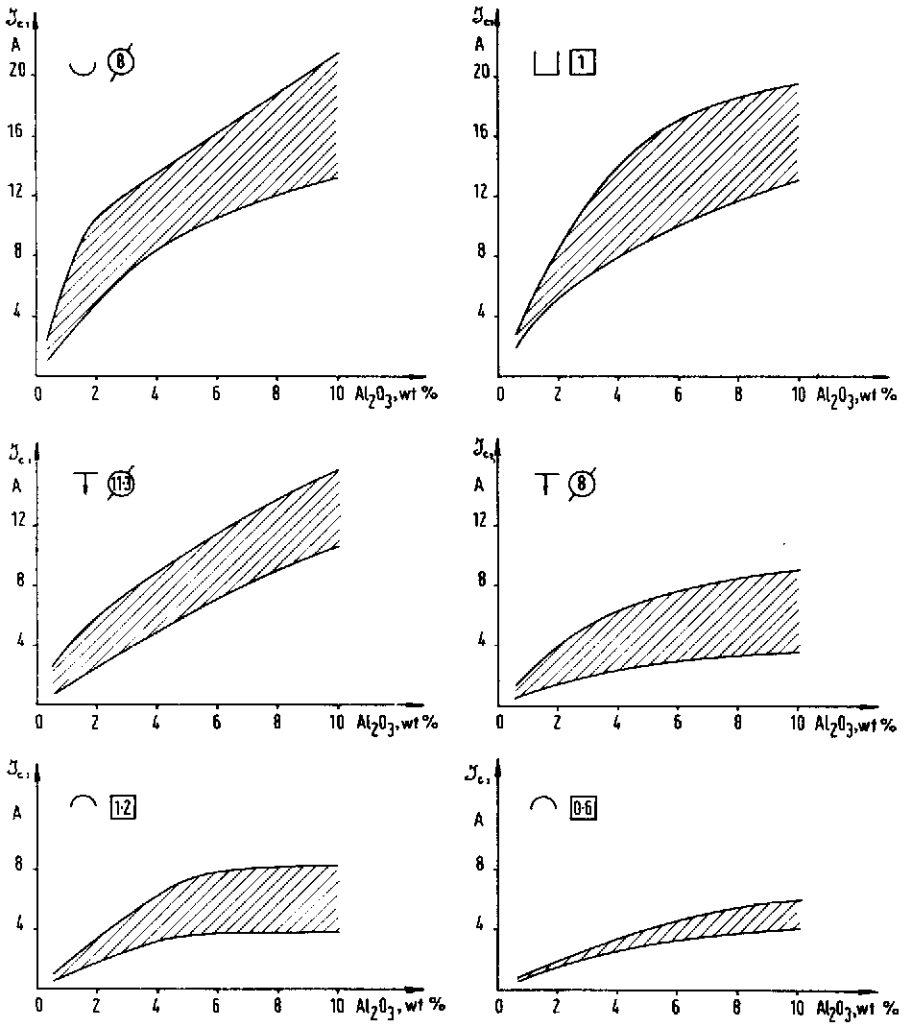

FIG. 11. Critical current intensity *vs* wt-% Al_2O_3 for various shapes and sizes of anodes. 1050°C.

scattered in a wide range, depending on current increasing law, history of the anodes, and other factors, such as the uncertain definition of the bath composition, etc.

As far as the influence of the bath "acidity" is concerned, the addition of AlF_3 lowers $\mathscr{T}_c$. Moreover, $\mathscr{T}_c$ increases with the increasing bath temperature (it increases about 1·5 times from 1000°C to 1150°C).

The results quoted above can be summarized (for cryolite-alumina melts) by assuming for the "critical current intensity" a law of dependence on the main factors having the form

$$\mathscr{T}_c \triangleq \psi \cdot f_1(T) \cdot f_2(A) \cdot f_3([Al_2O_3]),$$

or, more explicitly,

$$\mathscr{T}_c \triangleq \psi \cdot \{a + bT\} \cdot A^n \cdot \{c + [Al_2O_3]^m\},$$

TABLE 1. VALUES OF ψ FOR VARIOUS ANODE SHAPES

Anode shape	ψ
Horizontal (downwards)	1
Hemispherical	1·4
Cylindrical	1·3
Concave	0·5–0·55

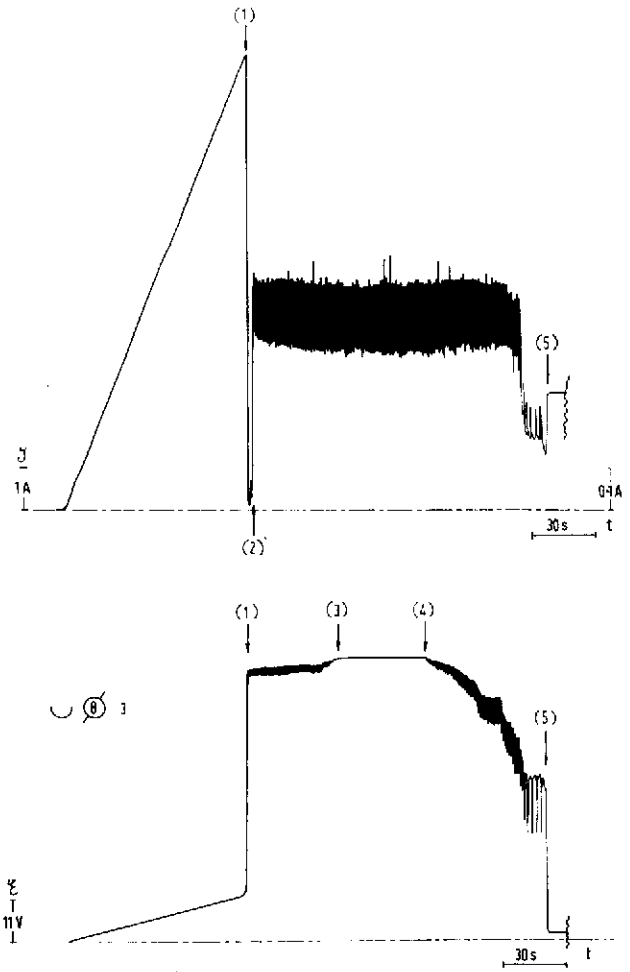

FIG. 12. Current and anode voltage in AE conditions. 1050°C.
(1) onset of the AE; the external resistance R^e is decreased up to (3);
(2) scale change;
(3) $R^e \simeq 0$;
(4) now R^e is increased till the AE disappears in (5).

where T is the bath temperature, A the electrode apparent area, $[Al_2O_3]$ the Al_2O_3 content of the baths, ψ a factor that depends only on the anode shape, and a, b, c, n, m are constants ($n < 1$; $m \simeq 0{\cdot}5$).

Numerically, for T in °C, A in cm², $[Al_2O_3]$ in wt-% (referred to Na_3AlF_6), and $\mathscr{T}_e$ in A, the following expression is obtained:

$$\mathscr{T}_e = \psi \cdot \{5{\cdot}5 + 1{\cdot}8 \times 10^{-2}(T - 1050)\} \times A^{0{\cdot}9} \times \{-0{\cdot}4 + [Al_2O_3]^{0{\cdot}5}\},$$

the values of ψ for various anode shapes being those indicated in Table 1.

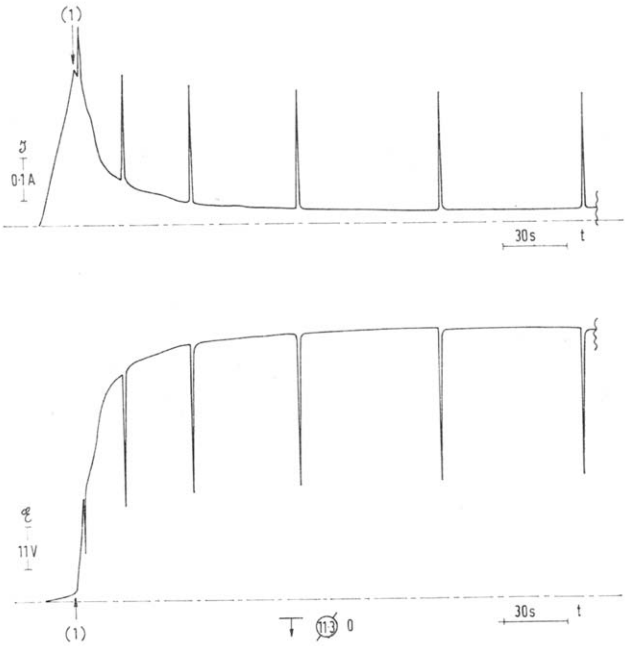

FIG. 13. Current and anode voltage in AE conditions. 1050°C.
(1) onset of the AE; then R^e kept constant.

This law is valid in the $[Al_2O_3]$ range 1–10 wt-% (referred to Na_3AlF_6) and in the temperature range 1000–1150°C, and it fits the experimental results in our laboratory conditions; it can be extended with reasonable approximation to industrial conditions.

Mechanical vibration impressed on the anodes increases $\mathscr{T}_e$ to a greater extent for the horizontal (downwards) and concave anodes than for the hemispherical and cylindrical ones of identical apparent area.

Some typical aspects of the onset and permanence of the AE are illustrated in Figs 12, 13 and 14. The phenomenology of the AE after its onset depends again on the shape and the history of the anodes and also on the power-supply conditions. The characteristic "bands" in the oscillographic recordings of current or anode voltage in AE conditions (Fig. 14) are always accompanied by the formation at the anode surface of a very bright arc and a considerable local increase of temperature. A systematic direct observation of these aspects of the AE has been performed with fused chloride baths, through the possibility of operating with transparent cells.

The disappearance of the AE is strongly influenced by the shape and the history of the anodes. The disappearance is easier for those anodes (cylindrical and hemispherical) that permit an easier evolution of the anode gas. Mechanical vibration impressed on the anodes in any case enhances the disappearance of the AE.

The main purpose of the work described has been to obtain a better knowledge of the phenomenological laws, and to look for still unexplored factors.

For given power-supply conditions and bulk composition of the bath, the circumstances determining the AE seem to be the physical–chemical characteristics of the interphase region and those of the gaseous phase, which decide whether it displaces the electrolyte in contact with the anode surface. The wetting properties of the anode surface are obviously important. On the other hand, the dynamic aspects of the AE, such as its abrupt onset, the oscillatory phenomena etc, could hardly be realized by considering merely changes in time of the wetting properties, on the basis of an essentially static concept such as the contact angle. We shall therefore proceed to a theoretical treatment following essentially dynamical lines. Meanwhile, further details and discussion will be found elsewhere.[4]

REFERENCES

1. R. PIONTELLI, *Chimica Ind.* **22**, 501 (1940); *J. Chim. Phys.* **49**, 29 (1952); *Alluminio* **22**, 731 (1953); R. PIONTELLI and G. MONTANELLI, *J. Chem. Phys.* **22**, 1781 (1954). R. PIONTELLI, G. MONTANELLI and G. STERNHEIM, *Revue Métall. Paris* **53**, 248 (1956). R. PIONTELLI and G. MONTANELLI, *Alluminio*, **25**, 79 (1956). R. PIONTELLI, *Rc. Ist. Lomb. Sci. Lett.* **92**, 367 (1958); *R.C. Accad. Lincei* **26**, 18 (1959); *Ann. N.Y. Acad. Sci.* **79**, 1025 (1960); *Metallurgia Ital.* **52**, 469 (1960); *Metallurgia Ital.* **52**, 478 (1960); *Proc. 1st Australian Conference on Electrochemistry, Sydney* (1963), p. 932. Pergamon Press, Oxford (1964).
2. S. I. REMPELL and L. P. KHODAK, *Zh. Prikl. Khim.* **26**, 931 (1953). W. E. HAUPIN, *J. Electrochem. Soc.* **103**, 174 (1956). H. STERN and G. T. HOLMES, *J. Electrochem. Soc.* **105**, 478 (1958). V. P. MASHOVETS and A. A. REVAZYAN, *Zh. Prikl. Khim.* **31**, 571 (1958). S. I. REMPELL, *The Anode Process in the Electrolytic Production of Aluminium*. Metallurgy Press, Moscow (1961). B. J. WELCH and N. E. RICHARDS, *AIME International Symposium on the Extractive Metallurgy of Aluminium, New York* (1962), Vol. 2, p. 15. Interscience, New York (1963). J. THONSTAD, *J. Electrochem. Soc.* **111**, 959 (1964).
3. V. SCHISCHKIN, *Z. Elektrochem.* **33**, 83 (1927). K. ARNDT and H. PROBST, *Z. Elektrochem.* **29**, 323 (1923). K. ARNDT, *Z. Elektrochem.* **33**, 236 (1927). FINKELSTEIN, *Lëgk. Metally*, July–August 1937, p. 24. V. P. MASHOVETS, *L'Electrométallurgie de l'Aluminium, ONTI* (1938). H. VON WARTENBERG, *Z. Elektrochem.* **32**, 330 (1926); *Z. Elektrochem.* **33**, 526 (1927). A. I. BELYAEV, M. B. RAPOPORT and L. A. FIRSANOVA, *Metallurgie des Aluminiums*, VEB Verlag Technik, Berlin (1956). A. I. BELYAEV, E. A. ZHEMCHUZHINA and L. A. FIRSANOVA, *Physical Chemistry of Fused Salts*. Metallurgy Press, Moscow (1957). A. VAJNA, *Bull. Soc. Fr. Electns*, **14**, 85 (1952). L. N. ANTIPIN and N. G. TURIN, *Zh. Fiz. Khim.* **31**, 1103 (1957). Y. YOSHIZAWA and N. WATANABE, CITCE 15th Meeting, London (1964), in press. H. H. KELLOGG, *J. Electrochem. Soc.* **97**, 133 (1950).
4. R. PIONTELLI, B. MAZZA and P. PEDEFERRI, *R.C. Accad. Lincei*, **36**, 759 (1964); **37**, 3 (1964). *Metallurgia Ital.*, **57**, 51 (1965).